

An improved lattice hydrodynamic model considering the “backward looking” effect and the traffic interruption probability

Changtao Jiang · Rongjun Cheng · Hongxia Ge

Received: 29 March 2017 / Accepted: 23 October 2017 / Published online: 7 November 2017
© Springer Science+Business Media B.V., part of Springer Nature 2017

Abstract By incorporating the “backward looking” effect and traffic interruption probability, we put forward an improved lattice model. Applying linear stability analysis, linear stability criterion is derived. The mKdV equation is deduced through nonlinear theory, which demonstrates that the solution of mKdV equation can describe traffic congestion. Furthermore, numerical simulation shows that the two factors can enhance traffic flow stability in the driving process.

Keywords Traffic flow · mKdV equation · Traffic interruption probability · “Backward looking” effect

1 Introduction

Recently, due to the serious traffic problems with the growing number of vehicles on the road, traffic jam problem has increasingly captured the attention

of scholars with different backgrounds. Consequently, plenty of traffic flow models have been constructed [1–7] to solve the traffic problems, including car-following models [8–16], cellular automation models [17–21], macro-traffic models [22–26] and lattice hydrodynamic models [27, 28]. Nagatani [29] firstly developed a lattice hydrodynamic model. What’s more, the mKdV equation is derived by Nagatani’s original lattice hydrodynamic model. Later, an increasing number of novel lattice hydrodynamic models [30–43] have been proposed by taking the other factors into consideration such as “backward looking” effect, driver’s memory during a period of time, driver’s desired average flux and traffic interruption probability.

In recent years, many scholars have taken into account the effect of the traffic interruption probability. Tang et al. [44, 45] considered this factor in traffic flow models. Subsequently, by considering the factor, Redhu and Gupta [46] derived a novel lattice hydrodynamic model. Furthermore, Peng et al. [47] and Sun et al. [48] researched this factor in lattice hydrodynamic model. However, the “backward looking” effect wasn’t taken into consideration in these models.

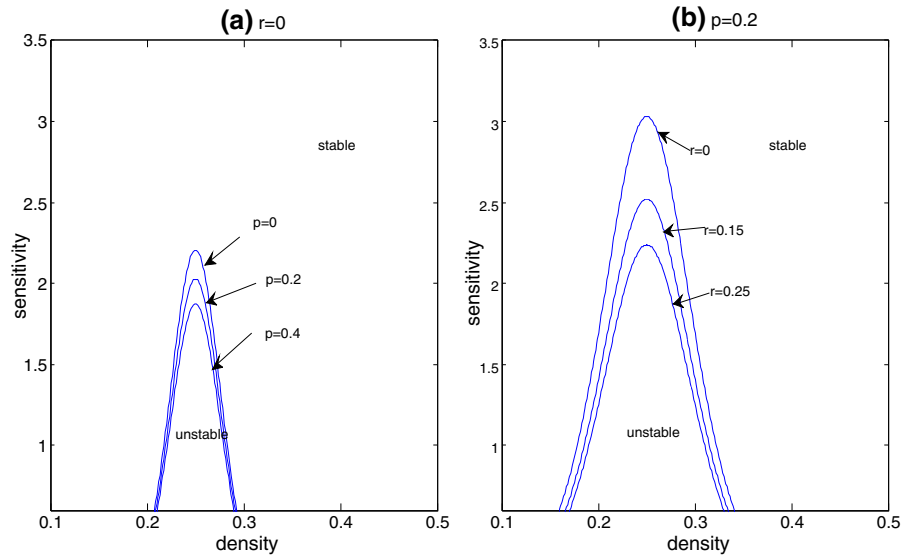
In this paper, the extended lattice hydrodynamic model is formulated by incorporating the “backward looking” effect and the influence of traffic interruption probability. The new model will be presented in the following section. The linear and nonlinear analyses of the new model are carried out in Sects. 2 and 3, respectively. Section 4 explores numerical simulations, and Sect. 5 draws conclusions.

C. Jiang · R. Cheng (✉) · H. Ge
Faculty of Maritime and Transportation, Ningbo University, Ningbo 315211, China
e-mail: chengrongjun@nbu.edu.cn

C. Jiang · R. Cheng · H. Ge
Jiangsu Province Collaborative Innovation Center for Modern Urban Traffic Technologies, Nanjing 210096, China

C. Jiang · R. Cheng · H. Ge
National Traffic Management Engineering and Technology Research Centre Ningbo University Sub-centre, Ningbo 315211, China

Fig. 1 Phase diagram in parameter space (ρ, a)



2 The extended lattice hydrodynamic model

On the basis of original lattice hydrodynamic model, an extended model is put forward by incorporating the “backward looking” effect and traffic interruption probability as follows:

$$\begin{aligned} &\rho_j(t + \tau)v_j(t + \tau) \\ &= \rho_o V_F(\rho_{j+1}(t)) + \lambda_1 p_{j+1} \cdot H(\bar{\rho} - \rho_{j-1}(t)) \\ &\quad \times H(\rho_{j-1}(t) - \rho_c) \cdot \rho_o V_B(\rho_{j-1}(t)) \\ &\quad + (1 - p_{j+1})\lambda_2(\rho_{j+1}v_{j+1} - \rho_j v_j), \end{aligned} \tag{1}$$

$$\partial t \rho_j + \rho_o(\rho_j v_j - \rho_{j-1} v_{j-1}) = 0, \tag{2}$$

where $H(\cdot)$ represents the Heaviside function, $\bar{\rho}$ is approaching to 1 and ρ_c indicates safety density. If $\bar{\rho}$ is less than the density, the “backward looking” influence will not play its role. Furthermore, as the safety density is greater than the density, the “backward looking” influence will also not play its role. τ represents the delay time and $a = \frac{1}{\tau}$ is the sensitivity. λ_1 and λ_2 are two reactive coefficients and p_{j+1} represents the interruption of lattice $j + 1$.

Here the coefficients g_i are given in Table 2.

For convenience, p_{j+1} is chosen as a constant p . The “forward looking” optimal velocity function is chosen as

$$\begin{aligned} V_F(\rho_{j+1}) &= \tanh\left(\frac{2}{\rho_o} - \frac{\rho_{j+1}(t)}{\rho_o^2} - \frac{1}{\rho_c}\right) \\ &\quad + \tanh\left(\frac{1}{\rho_c}\right), \end{aligned} \tag{3}$$

and the “backward looking” optimal velocity function is as follows:

$$\begin{aligned} V_B(\rho_{j-1}) &= r \left[-\tanh\left(\frac{2}{\rho_o} - \frac{\rho_{j+1}(t)}{\rho_o^2} - \frac{1}{\rho_c}\right) \right. \\ &\quad \left. + \tanh\left(\frac{1}{\rho_c}\right) \right], \end{aligned} \tag{4}$$

where ρ_o represents the initial density and r represents a positive constant. We set $r = 0.15, 0.25, 0.4$, respectively. Eliminating speed v in Eqs. (1) and (2), we will derive

$$\begin{aligned} &\rho_j(t + 2\tau) - \rho_j(t + \tau) + \tau \rho_o^2 \\ &\quad \left[V_F(\rho_{j+1}(t)) - V_F(\rho_j(t)) + \lambda_1 p (V_B(\rho_{j-1}(t)) \right. \\ &\quad \left. - V_B(\rho_{j-2}(t))) \right] \\ &\quad + (1 - p)\lambda_2 [\rho_{j+1}(t) - \rho_{j+1}(t + \tau) \\ &\quad + \rho_j(t + \tau)\rho_j(t)]. \end{aligned} \tag{5}$$

We investigate the BL-LH model with the linear stability analysis. The steady-state solution for Eqs. (1) and (2) is given as:

$$\rho_j(t) = \rho_o, \tag{6}$$

$$v_j(t) = V_F(\rho) + V_B(\rho), \tag{7}$$

y_j is a small perturbation of traffic flow from the steady-state flow as

$$\rho_j(t) = \rho_o + y_j(t). \tag{8}$$

Table 1 Coefficients k_i of the model

k_1	k_2
$b + \rho_o^2 V_F(\rho_c)' + \rho_o^2 \lambda_1 p V_B(\rho_c)'$	$\frac{3}{2} b^2 \tau_c + \frac{\rho_o^2 V_F(\rho_c)' - 3 \rho_o^2 \lambda_1 p V_B(\rho_c)'}{12} - \lambda_2 (1 - p)$
k_4	k_6
$\frac{\rho_o^2 V_F(\rho_c)''' + \rho_o^2 \lambda_1 p V_B(\rho_c)'''}{6}$	$\frac{15 b^4 \tau_c^3 + \rho_o^2 V_F(\rho_c)' - 15 \rho_o^2 \lambda_1 p V_B(\rho_c)' - 2 \lambda_2 (1 - p) (4 b + 6 b \tau_c + 4 b \tau_c^3)}{24}$
k_5	k_3
$3 b \tau_c - \lambda_2 (1 - p)$	$\frac{7 b^3 \tau_c^2 + \rho_o^2 V_F(\rho_c)'}{6} - \frac{\lambda_2 (1 - p) (b + b^2 \tau_c)}{2}$
k_7	
$\frac{\rho_o^2 V_F(\rho_c)''' - 3 \rho_o^2 \lambda_1 p V_B(\rho_c)'''}{12}$	

Table 2 Coefficients g_i of the model

g_1	g_2	g_3
$\frac{7 b^3 \tau_c^2 + \rho_o^2 V_F(\rho_c)'}{6} - \frac{\lambda_2 (1 - p) (b + b^2 \tau_c)}{2}$	$\frac{\rho_o^2 V_F(\rho_c)''' + \rho_o^2 \lambda_1 p V_B(\rho_c)'''}{6}$	$3 b^2 \tau_c$
g_4	g_5	
$\frac{15 b^4 \tau_c^3 + \rho_o^2 V_F(\rho_c)' - 15 \rho_o^2 \lambda_1 p V_B(\rho_c)' - 2 \lambda_2 (1 - p) (4 b + 6 b \tau_c + 4 b \tau_c^3)}{24}$	$\frac{\rho_o^2 V_F(\rho_c)''' - 3 \rho_o^2 \lambda_1 p V_B(\rho_c)'''}{12}$	

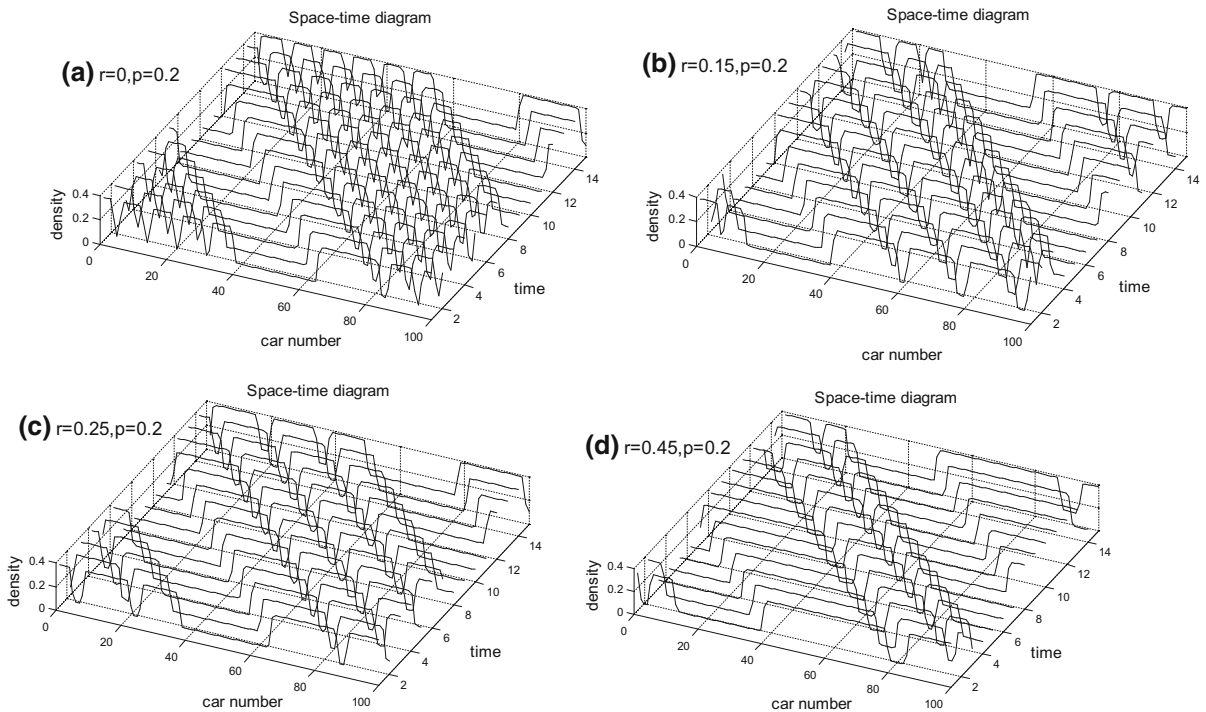


Fig. 2 Phase diagram of the model according to different values of parameter p

Inserting Eq. (6) into (5), we will deduced

$$y_j(t + 2\tau) - y_j(t + \tau) + \tau \rho_o^2 [V_F(\rho_o)'(y_{j+1}(t) - y_j(t))$$

$$+ \lambda_1 p V_B(\rho_o)'(y_{j-1}(t) - y_{j-2}(t))] + (1 - p) \lambda_2 [y_{j+1}(t) - y_{j+1}(t + \tau) + y_j(t + \tau) - y_j(t)]. \tag{9}$$

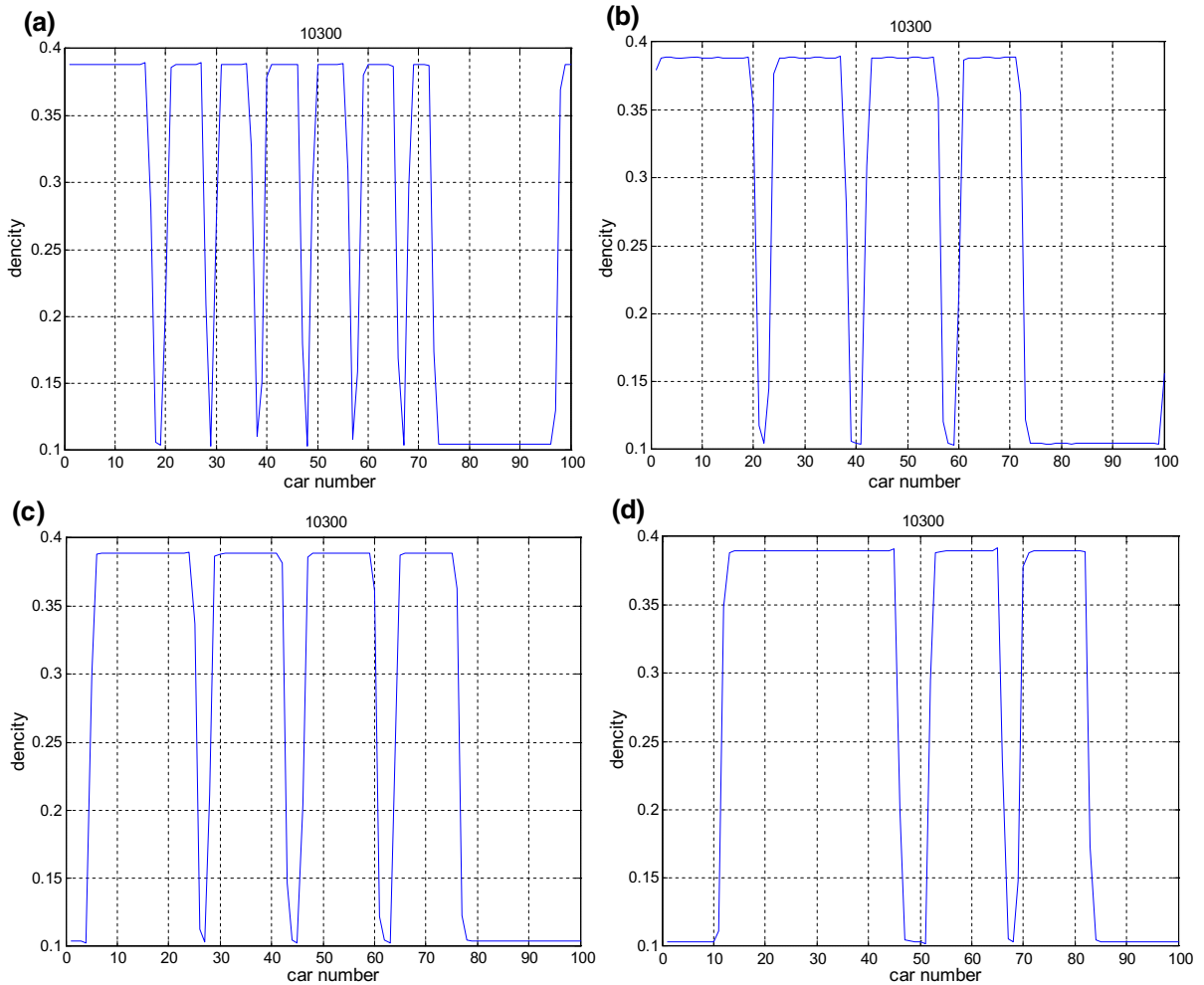


Fig. 3 Headway profile at $t = 10,300$ under the different value of p

Expanding $y_j = \exp(ikj + zt)$, it reads:

$$e^{2z\tau} - e^{z\tau} + \tau\rho_o^2 \left[V_F(\rho_o)'(e^{ik} - 1) + \lambda_1 p V_B(\rho_o)'(e^{-ik} - e^{-2ik}) \right] + (1 - p)\lambda_2(e^{ik} - e^{ik+z\tau} + e^{z\tau} - 1) = 0, \tag{10}$$

where $V(\rho_o)' = \frac{dV_\rho}{d\rho|_{\rho=\rho_o}}$. Let $z = z_1(ik) + z_2(ik)^2 + \dots$, then the first-order and second-order terms of ik are:

$$z_1 = -\rho_o^2 [V_F(\rho_o)' + \lambda_1 p V_B(\rho_o)'], \tag{11}$$

$$z_2 = \rho_o^2 \left[\frac{V_F(\rho_o)' - 3\lambda_1 p V_B(\rho_o)'}{2} + \lambda_2(V_F(\rho_o)' + \lambda_1 p V_B(\rho_o)') \right] - \frac{3}{2}\tau [V_F(\rho_o)' + \lambda_1 p V_B(\rho_o)']^2. \tag{12}$$

The stability of traffic flow is determined by the value of z_2 for long wavelengths. The stable traffic flow will become unstable when $z_2 < 0$, but keep stable when $z_2 > 0$. Therefore, one acquires the neutral stability condition as below:

$$\tau = \frac{\frac{1}{2} [V_F(\rho_o)' - 3\lambda_1 p V_B(\rho_o)'] + (1 - p)\lambda_2 [V_F(\rho_o)' + \lambda_1 p V_B(\rho_o)']}{-\frac{3}{2}\rho_o^2 [V_F(\rho_o)' + \lambda_1 p V_B(\rho_o)']^2}. \tag{13}$$

The stability condition is given:

$$\tau < \frac{\frac{1}{2} [V_F(\rho_o)' - 3\lambda_1 p V_B(\rho_o)'] + (1 - p)\lambda_2 [V_F(\rho_o)' + \lambda_1 p V_B(\rho_o)']}{-\frac{3}{2}\rho_o^2 [V_F(\rho_o)' + \lambda_1 p V_B(\rho_o)']^2}. \tag{14}$$

The phase diagram in the (ρ, a) —plane is described in Fig. 1 where ρ is the density and a is sensitivity. The

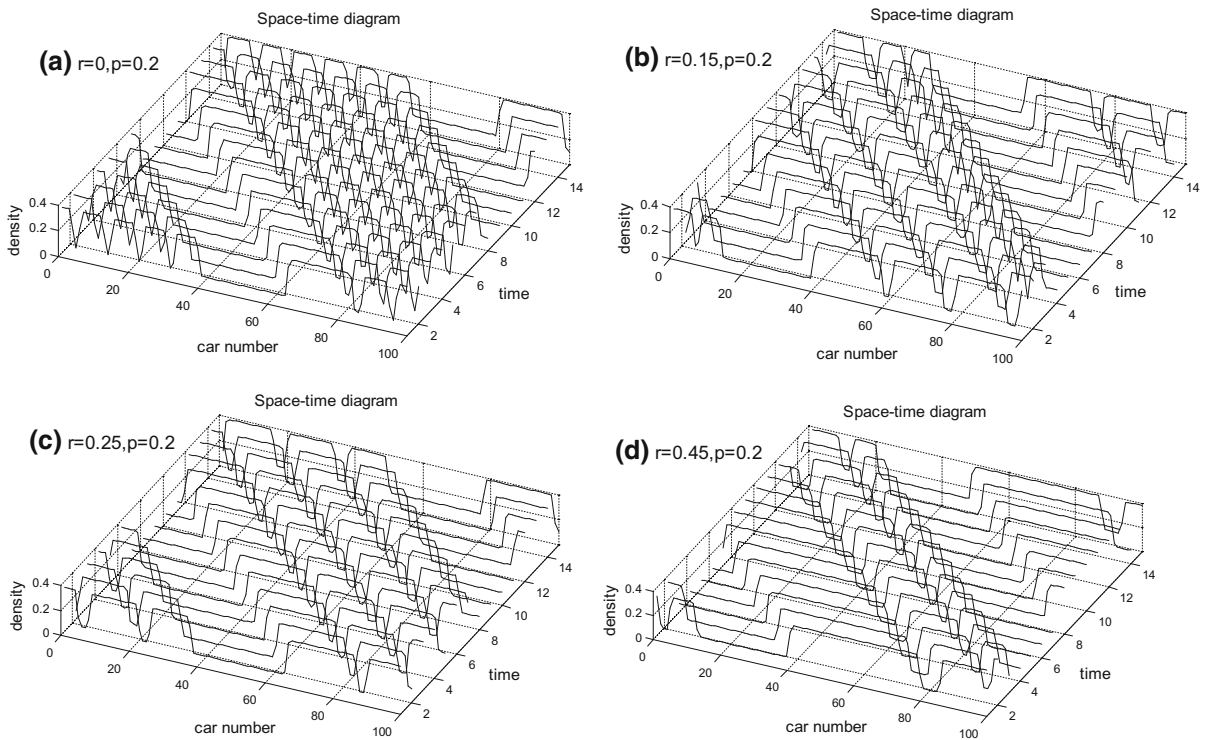


Fig. 4 Phase diagram of the model according to different values of parameter r

stability curves are shown as solid lines indicate. If the value of the parameter ρ or r decreases, the critical points will rise. Different parameter indicates the simulation results. Thus, we can conclude that the of traffic stability is enhanced with consideration of the “backward looking” effect and the influence of the traffic interruption probability.

3 mKdV equation

The modified KdV equations will be derived to describe the slowly varying behaviors for long waves near the critical point (ρ_c, a_c) . For the space variable n and the time t , define the slow variables X and T as follows:

$$X = \varepsilon(j + bt), T = \varepsilon^3 t, \rho_j = \rho_c + \varepsilon R(X, T), \tag{15}$$

where $0 < \varepsilon \ll 1$ and b is a constant to be determined. By inserting Eq. (13) into (5) and expanding each term in Eq. (5) to the fifth order of ε by substituting, one obtains:

$$\begin{aligned} &\varepsilon^2 k_1 \partial_X R + \varepsilon^3 k_2 \partial_X^2 R \\ &+ \varepsilon^4 (\partial_T^R + k_3 \partial_X^3 R + k_4 \partial_X R^3) \\ &+ \varepsilon^5 (k_5 \partial_T \partial_R + k_6 \partial_X^4 R + k_7 \partial_X^2 R^3) = 0. \end{aligned} \tag{16}$$

By inserting $b = -\rho_c^2 (V_F(\rho_c)' + \lambda_1 p V_B(\rho_c)')$, $\tau = (1 + \varepsilon^2)\tau_c$ into Eq. (14), one obtains:

$$\begin{aligned} &\varepsilon^4 (-g_1 \partial_X^3 R + g_2 \partial_X R^3 + \partial_T R) \\ &+ \varepsilon^5 (g_4 \partial_X^4 R + g_5 \partial_X^3 R^3 + g_3 \partial_X^2 R) = 0. \end{aligned} \tag{17}$$

Here the coefficients k_i are given in Table 1.

In the table, $V' = dV(\rho)/d\rho|_{\rho = \rho_c}$, $V''' = d^3V(\rho)/d\rho^3|_{\rho = \rho_c}$. To obtain the regularized equation, transformation is made as follows:

$$T = \frac{1}{g_1} T', R = \sqrt{\frac{g_1}{g_2}}. \tag{18}$$

We can obtain the modified mKdV equation with an $O(\varepsilon)$ correction term as follows:

$$\begin{aligned} &\partial_{T'} R' = \partial_X^3 R' - \partial_X R'^3 \\ &+ \varepsilon \left[\frac{g_3}{g_1} \partial_X^2 R' + \frac{g_4}{g_1} \partial_X^4 R' + \frac{g_5}{g_2} \partial_X^2 R'^3 \right]. \end{aligned} \tag{19}$$

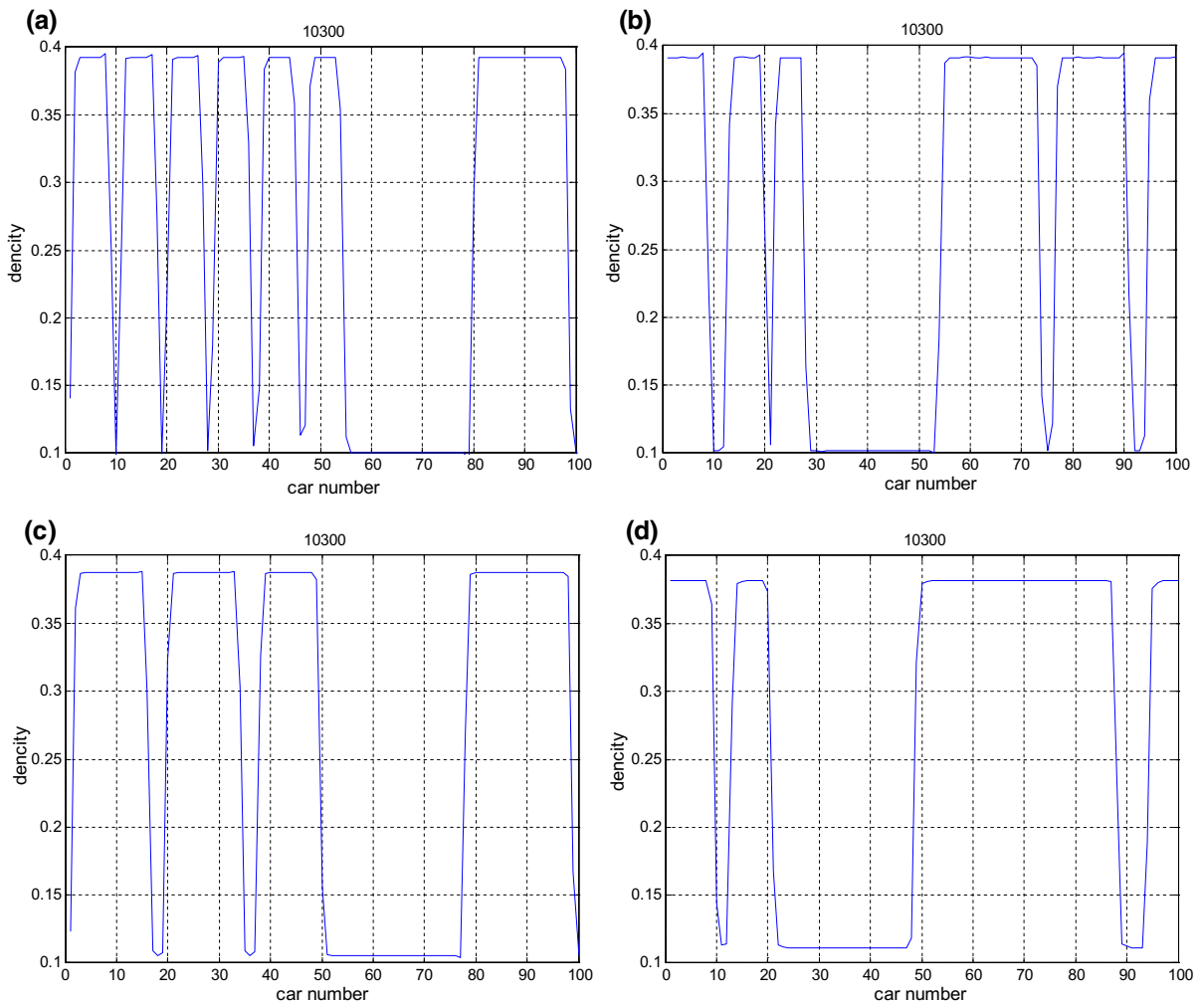


Fig. 5 Headway profile at $t = 10,300$ under the different value of r

We get the mKdV equations with a kink solution after ignoring the $O(\varepsilon)$:

$$R'_o(X, T') = \sqrt{c} \tanh \sqrt{\frac{c}{2}}(X - cT'). \tag{20}$$

Then, the $O(\varepsilon)$ correction is considered by assuming $R'_o(X, T') = R'_o(X, T') + \varepsilon R'_1(X, T')$. For the purpose of obtaining the propagation velocity c for the kink solution, the solvability condition should be satisfied. $(R'_o, M[R'_o]) \equiv \int_{-\infty}^{+\infty} dX' R'_o M[R'_o]$, where $M[R'_o] = \frac{g_3}{g_1} \partial_X^2 R' + \frac{g_4}{g_1} \partial_X^4 R' + \frac{g_1 g_5}{g_1} \partial_X^2 R'^3$. We get the general velocity c :

$$c = \frac{5g_2g_3}{2g_2g_4 - 3g_1g_5}. \tag{21}$$

Subsequently, the general kink–antikink solution of the mKdV equation can be obtained:

$$\rho_j(t) = h_c \pm \sqrt{\frac{g_1c}{g_2} \left(\frac{\tau}{\tau_c} - 1\right)} \times \tanh \sqrt{\frac{c}{2} \left(\frac{\tau}{\tau_c} - 1\right)} \times \left[j + (1 - cg_1) \left(\frac{\tau}{\tau_c} - 1\right) t \right] \tag{22}$$

4 Numerical simulation

In this section, the effect of “backward looking” and traffic interruption probability is investigated by numerical simulation. The boundary condition is chosen to be periodic. The initial condition is chosen as follows:

$\rho_j(0) = \rho_o = 0.25$, $\rho_j(1) = \rho_o = 0.25$, for $j \neq 50, 51$, $\rho_j(1) = 0.25 - 0.1$, for $j = 50$, $\rho_j(1) = 0.25 + 0.1$, for $j = 51$. The total number of sites and the sensitivity are chosen as $N = 100$ and $a = 1.25$.

The simulation patterns of the density with different value of r ($p = 0.2$) are described after time $t = 10^4$ s in Fig. 2. From pattern (a) with $r = 0$, it confirms Peng's model [47]. It is clear that the changes in the density become stranger than others. With a small disturbance, the initial steady traffic flow will turn into stop and go traffic waves, which is similar to the mKdV solution. With the increase in r , the scales of density waves is not large. The patterns of the density after $t = 10^4$ s with different value of p ($r = 0.2$) are demonstrated in Fig. 4. With the increase in r , the changes in density reduce gradually. In conclusion, traffic flow stability can be improved efficiently with the consideration of the influence of the traffic interruption probability and "backward looking" effect.

Figures 3 and 5 reveal the density profile corresponding to Figs. 2 and 4 at $t = 10,300$ s. So, the simulation results are in agreement with the theoretical analysis.

5 Conclusion

A novel lattice hydrodynamic model has been put forward by taking into account the "backward looking effect" and the influence of the traffic interruption probability. With the theory of the linear and nonlinear analyses, the traffic properties have been analyzed. We have obtained the stability of the model. To describe the traffic congestion, we have derived the mKdV equation. The numerical results is consistent with nonlinear analysis for the extended traffic model. Ge and Cheng [37] also considered the "backward looking" effect in lattice hydrodynamic model for the purpose of suppressing the traffic congestion. On the basis of Ge's model, traffic interruption probability has been added in this paper. Compared with Ge's model, we can see the changes in density reduce faster from the numerical simulation in this paper. This means traffic flow in this paper is more stable than Ge's model. Therefore, the influence of the traffic interruption probability and "backward looking" effect can improve efficiently the stability of the traffic flow.

Acknowledgements This work is supported by the National Natural Science Foundation of China (Grant Nos. 71571107,

61773290, 11702153), the Natural Science Foundation of Zhejiang Province, China (Grant Nos. LY18A010003, LY16G010003), and the K. C. Wong Magna Fund in Ningbo University, China.

Compliance with ethical standards

Conflict of interest The authors declare that there is no conflict of interests regarding the publication of this article.

References

1. Bando, M., Hasebe, K., Nakayama, A., Shibata, A., Sugiyama, Y.: Dynamics model of traffic congestion and numerical simulation. *Phys. Rev. E* **51**, 1035–1042 (1995)
2. Nagatani, T.: The physics of traffic jams. *Rep. Prog. Phys.* **65**, 1331–1386 (2002)
3. Jiang, R., Wu, Q.S., Zhu, Z.J.: A new continuum model for traffic flow and numerical tests. *Trans. Res. B* **36**, 405–419 (2002)
4. Jiang, R., Hu, M.B., Zhang, H.M., Gao, Z.Y., Jia, B., Wu, Q.S.: On some experimental features of car-following behavior and how to model them. *Transp. Res. Part B* **80**, 338–354 (2015)
5. Xue, Y.: Analysis of the stability and density waves for traffic flow. *Chin. Phys.* **11**, 1128–1134 (2002)
6. Ge, H.X., Dai, S.Q., Xue, Y., Dong, L.Y.: Stabilization analysis and modified Korteweg–de Vries equation in a cooperative driving system. *Phys. Rev. E* **71**, 066119 (2005)
7. Cheng, R.J., Ge, H.X., Wang, J.F.: An extended continuum model accounting for the driver's timid and aggressive attributions. *Physica A* **381**, 1302–1312 (2017)
8. Tang, T.Q., Li, J.G., Wang, Y.P., Yu, G.Z.: Vehicle's fuel consumption of car-following models. *Sci. China Technol. Sci.* **56**, 1307–1312 (2013)
9. Tang, T.Q., Wang, Y.P., Yang, X.B., Wu, Y.G.: A new car-following model accounting for varying road condition. *Nonlinear Dyn.* **70**, 1397–1405 (2012)
10. Tang, T.Q., Shi, Y.F., Wang, Y.P., Yu, G.Z.: A bus-following model with an on-line bus station. *Nonlinear Dyn.* **70**, 209–215 (2012)
11. Tang, C.F., Jiang, R., Wu, Q.S., Wiwatanapataphee, B., Wu, Y.H.: Mixed traffic flow in anisotropic continuum model. *Transp. Res. Rec.* **1999**, 13–22 (2007)
12. Sun, D.H., Zhang, M., Chuan, T.: Multiple optimal current difference effect in the lattice traffic flow model. *Mod. Phys. Lett. B* **28**, 1450091 (2014)
13. Tang, T.Q., Shi, W.F., Shang, H.Y., Wang, Y.P.: A new car-following model with consideration of inter-vehicle communication. *Nonlinear Dyn.* **76**, 2013–2017 (2014)
14. Li, Z.P., Xu, X., Xu, S.Z., Qian, Y.Q., Xu, J.: Analytical studies on an extended car following model for mixed traffic flow with slow and fast vehicles. *Int. J. Mod. Phys. C* **27**, 1650004 (2016)
15. Peng, G.H., Lu, W.Z., He, H.D., Gu, Z.H.: Nonlinear analysis of a new car-following model accounting for the optimal velocity changes with memory. *Commun. Nonlinear Sci. Numer. Simul.* **40**, 197–205 (2016)

16. Song, H., Ge, H.X., Chen, F.Z., Cheng, R.J.: TDGL and mKdV equations for car-following model considering traffic jerk and velocity difference. *Nonlinear Dyn.* **87**, 1809–1817 (2017)
17. Moussa, N., Daoudia, A.K.: Numerical study of two classes of cellular automaton models for traffic flow on a two-lane roadway. *Eur. Phys. B* **31**, 413–420 (2003)
18. Xue, S.Q., Jia, B., Jiang, R.: A behaviour based cellular automaton model for pedestrian counter flow. *J. Stat. Mech. Theory Exp.* **2016**, 113204 (2016)
19. Das, S.: Cellular automaton based traffic model that allows the cars to move with a small velocity during congestion. *Chaos Solitons Fractals* **44**, 185–190 (2011)
20. Chmura, T., Herz, B., Knorr, F., Pitz, T., Schreckenberg, M.: A simple stochastic cellular automaton for synchronized traffic flow. *Physica A* **405**, 332–337 (2014)
21. Nagel, K., Schreckenberg, M.: A cellular automaton model for freeway traffic. *J. Phys. I* **2**, 212–229 (1992)
22. Tang, T.Q., Shi, W.F., Yang, X.B., Wang, Y.P., Lu, G.Q.: A macro traffic flow model accounting for road capacity and reliability analysis. *Physica A* **392**, 6300–6306 (2013)
23. Li, Y.F., Sun, D.H., Liu, W.N., Zhang, M., Zhao, M., Liao, X.Y., Tang, L.: Modeling and simulation for microscopic traffic flow based on multiple headway, velocity and acceleration difference. *Nonlinear Dyn.* **66**, 15–28 (2011)
24. Peng, G.H., Song, W., Peng, Y.J., Wang, S.H.: A novel macro model of traffic flow with the consideration of anticipation optimal velocity. *Physica A* **398**, 76–82 (2014)
25. Tang, T.Q., Huang, H.J., Shang, H.Y.: An extended macro traffic model accounting for the driver's bounded rationality and numerical tests. *Physica A* **468**, 322–333 (2017)
26. Goatin, P., Rossi, F.: A traffic flow model with non-smooth metric interaction: well-posedness and micro-macro limit. *Commun. Math. Sci.* **15**, 261–287 (2017)
27. Li, Z.P., Zhong, C.J., Chen, L.Z., XU, S.Z., Qian, Y.Q.: Analytical studies on a new lattice hydrodynamic traffic flow model with consideration of traffic current cooperation among three consecutive sites. *Int. J. Mod. Phys. C* **27**, 1650034 (2016)
28. Tian, J.F., Yuan, Z.Z., Jia, B., Li, M.H., Jiang, G.J.: The stabilization effect of the density difference in the modified lattice hydrodynamic model of traffic flow. *Physica A* **391**, 4476–4482 (2012)
29. Nagatani, T.: Modified KDV equation for jamming transition in the continuum models of traffic. *Physica A* **271**, 599–607 (1998)
30. Tang, T.Q., He, J., Wu, Y.H., Caccetta, L.: Propagating properties of traffic flow on a ring road without ramp. *Physica A* **396**, 164–172 (2014)
31. Li, Z.P., Xu, X., Xu, S.Z., Qian, Y.Q.: A heterogeneous traffic flow model consisting of two types of vehicles with different sensitivities. *Commun. Nonlinear Sci. Numer. Simul.* **42**, 132–145 (2017)
32. Li, Z.P., Li, W.Z., Xu, S.Z., Qian, Y.Q., Sun, J.: Traffic behavior of mixed traffic flow with two kinds of different self-stabilizing control vehicles. *Physica A* **436**, 729–738 (2015)
33. Ge, H.X., Cheng, R.J., Lo, S.M.: Time-dependent Ginzburg–Landau equation for lattice hydrodynamic model describing pedestrian flow. *Chin. Phys. B* **22**, 070507 (2013)
34. Peng, G.H., Qing, L.: The effects of drivers' aggressive characteristics on traffic stability from a new car-following model. *Mod. Phys. Lett. B* **30**, 1650243 (2016)
35. Lv, F., Zhu, H.B., Ge, H.X.: TDGL and mKdV equations for car-following model considering driver's anticipation. *Nonlinear Dyn.* **77**, 1245–1250 (2014)
36. Helbing, D., Tilch, B.: Generalized force model of traffic dynamics. *Phys. Rev. E* **58**, 133–138 (1998)
37. Ge, H.X., Cheng, R.J.: The “backward looking” effect in the lattice hydrodynamic model. *Physica A* **387**, 6952–6958 (2008)
38. Tian, H.H., Hu, H.D., Wei, Y.F., Xue, Y., Lu, W.Z.: Lattice hydrodynamic model with bidirectional pedestrian flow. *Physica A* **388**, 2895–2902 (2009)
39. Li, X.Q., Fang, K.L., Peng, G.H.: A new lattice model of traffic flow with the consideration of the drivers' aggressive characteristics. *Physica A* **468**, 315–321 (2017)
40. Yu, L., Li, T., Shi, Z.K.: Density waves in a traffic flow with reaction-time delay. *Physica A* **389**, 2607–2616 (2010)
41. Redhu, P., Gupta, A.K.: Phase transition in a two dimensional triangular flow with consideration of optimal current difference effect. *Nonlinear Dyn.* **78**, 957–968 (2014)
42. Zhou, J., Shi, Z.K., Cao, J.L.: An extended traffic flow model on a gradient highway with the consideration of the relative velocity. *Nonlinear Dyn.* **78**, 1765–1799 (2014)
43. Yang, S.C., Li, M., Tang, T.Q.: An electric vehicle's battery life model under car-following model. *Measurement* **46**, 4226–4231 (2013)
44. Tang, T.Q., Huang, H.J., Wong, S.C., Jiang, R.: A new car-following model with consideration of the traffic interruption probability. *Phys. B* **18**, 975–983 (2009)
45. Tang, T.Q., Huang, H.J., Xu, G.: A new macro model with consideration of the traffic interruption probability. *Physica A* **387**, 6845–6856 (2008)
46. Redhu, P., Gupta, A.K.: Jamming transitions and the effect of interruption probability in a lattice traffic flow model with passing. *Physica A* **421**, 249–260 (2015)
47. Peng, G.H., Lu, W.Z., He, H.D.: Impact of the traffic interruption probability of optimal current on traffic congestion in lattice model. *Physica A* **425**, 27–33 (2015)
48. Sun, D.H., Zhang, G., Liu, W.N.: Effect of explicit lane changing in traffic lattice hydrodynamic model with interruption. *Nonlinear Dyn.* **86**, 269–282 (2016)